# Singularities in triclinic anisotropy

Václav Vavryčuk

*Geophysical Institute, Academy of Sciences, Boční II/1401, 141 31 Praha 4, Czech Republic. E-mail: vv@ig.cas.cz*

**Abstract**

Triclinic elastic anisotropy contains at most 16 isolated singularities. The singularities can be in real or complex directions. If we count both real and complex singularities and their multiplicities, the total number of singularities is always 16 regardless of symmetry or strength of anisotropy. The real singularities describe the propagation of homogeneous plane waves, the complex singularities describe the propagation of inhomogeneous plane waves. The real singularities generate a linear polarization of waves in their vicinity. The complex singularities generate an elliptical polarization. The triclinic anisotropy with 6-10 real acoustic axes is most common. Examples of media with no or 16 real singularities are presented.

## 1. Introduction

Singularities (acoustic axes, degeneracies) in anisotropic elastic media are directions in which phase velocities of two or three plane waves coincide. These directions are important because they cause anomalies in the field of polarization vectors (Alshits & Lothe 1979a,b; Alshits et al. 1985; Shuvalov 1998), and they are associated with caustics in the wave surface (Every 1986, 1988; Shuvalov & Every 1997; Wolfe 1998; Vavryčuk 2003a). Singularities also pose complications in tracing rays and wavefield modeling (Vavryčuk 2003b).

The acoustic axes form single isolated points on the slowness surface or they can join into lines. The number of isolated acoustic axes in various anisotropy symmetries has been studied by many authors (Khatkevich 1963; Fedorov 1968; Musgrave 1985; Darinskij 1994; Boulanger & Hayes 1998, Mozhaev et al. 2001). They have shown that the maximum number is: 16 in monoclinic anisotropy, 16 in orthorhombic anisotropy, 13 in tetragonal symmetry, 10 in trigonal symmetry, and 7 in cubic symmetry. As regards triclinic anisotropy, Khatchevich (1963) showed that the acoustic axes can be calculated by solving two polynomial equations in two variables of the sixth order. This implies that the number of acoustic axes in triclinic anisotropy cannot exceed 36. However, Khatkevich (1963) did not discuss whether the actual maximum number of acoustic axes is less than 36 or not. Later on, Darinskij (1994) proved that typical triclinic crystals (when the S1 and S2 waves

are degenerate) cannot have more than 16 acoustic axes, and Holm (1992) showed that generic triclinic crystals possess also at most 16 acoustic axes.

In this paper, the following questions are addressed: What is the maximum number of acoustic axes under no restrictions on triclinic anisotropy? What is the connection between acoustic axes of homogeneous and inhomogeneous waves? What is the frequency of occurrence of acoustic axes in randomly generated triclinic media and how this frequency depends on strength of anisotropy?

## 2. Theory

The Christoffel tensor $\mathbf{\Gamma}(\mathbf{n})$ is defined as

$$\Gamma_{jk}(\mathbf{n}) = a_{ijkl} n_i n_l \ , \tag{1}$$

where $a_{ijkl}$ are the density-normalized elastic parameters and $\mathbf{n}$ is the unit vector defining the slowness direction. The Einstein summation convention over repeated subscripts is applied. The Christoffel tensor $\mathbf{\Gamma}(\mathbf{n})$ has three eigenvalues $G^{(M)}$ and three unit eigenvectors $\mathbf{g}^{(M)}$, which are calculated from

$$\Gamma_{jk} g_k^{(M)} = G^{(M)} g_j^{(M)} \ , M = 1,2,3 \ . \tag{2}$$

The eigenvalues correspond to squared phase velocities of the *P*, *S*1 and *S*2 waves propagating in anisotropic media, $G = c^2$, and the eigenvectors describe their polarization vectors. Using the spectral decomposition of $\mathbf{\Gamma}(\mathbf{n})$

$$\Gamma_{jk} = G^{(1)} g_j^{(1)} g_k^{(1)} + G^{(2)} g_j^{(2)} g_k^{(2)} + G^{(3)} g_j^{(3)} g_k^{(3)} , \tag{3}$$

and applying the condition for the acoustic axis, $G^{(2)} = G^{(3)}$, we obtain

$$\Gamma_{jk} = \left(G^{(1)} - G^{(2)}\right) g_j^{(1)} g_k^{(1)} + G^{(2)} \delta_{jk} , \tag{4}$$

where $\delta_{jk}$ is the Kronecker delta and we have used the following identity

$$\delta_{jk} = g_j^{(1)} g_k^{(1)} + g_j^{(2)} g_k^{(2)} + g_j^{(3)} g_k^{(3)} \ . \tag{5}$$

If $G^{(1)} > G^{(2)} = G^{(3)}$, the *S*1 and *S*2 phase velocities coincide at the acoustic axis (the so-called *S*1-*S*2 axis), if $G^{(1)} < G^{(2)} = G^{(3)}$, the *P* and *S*1 phase velocities coincide at the acoustic axis (the so-called *P*-*S*1 axis). Equation (4) can be rewritten as follows (see Darinskij 1994)

$$a_{ijkl} p_i p_l = g_j g_k + \delta_{jk} \ , \tag{6}$$

where $\mathbf{s} = \mathbf{n} / \sqrt{G^{(2)}}$ is the slowness vector of the degenerate wave and $\mathbf{g} = \mathbf{g}^{(1)} / \sqrt{G^{(1)} - G^{(2)}}$ is an eigenvector of the non-degenerate wave with a generally non-unit length. The vectors **s** and **g** can be complex-valued. Equation (6) is a system of six quadratic equations for six unknowns: $s_i$ and $g_i$, i=1,2,3. The number of solutions is $2^6 = 64$. If we take into account that solutions of different signs: $\pm s_i$, $\pm g_i$, define the same acoustic axis, the maximum number of acoustic axes is reduced from 64 to 16. This number comprises acoustic axes for homogeneous plane waves (slowness vector **s** is real-valued) as well as for inhomogeneous plane waves (slowness vector **s** is complex-valued).

Eliminating eigenvalues and eigenvectors in eq. (4), we obtain (Darinskij 1994)

$$\Gamma_{11} - \frac{\Gamma_{12}\Gamma_{13}}{\Gamma_{23}} = \Gamma_{22} - \frac{\Gamma_{12}\Gamma_{23}}{\Gamma_{13}} = \Gamma_{33} - \frac{\Gamma_{13}\Gamma_{23}}{\Gamma_{12}} \ , \tag{7}$$

or alternatively (Khatkevich 1963)

$$(\Gamma_{11} - \Gamma_{22})\Gamma_{13}\Gamma_{23} - \Gamma_{12}(\Gamma_{13}^2 - \Gamma_{23}^2) = 0 \ , \tag{8a}$$

$$(\Gamma_{11} - \Gamma_{33})\Gamma_{12}\Gamma_{23} - \Gamma_{13}(\Gamma_{12}^2 - \Gamma_{23}^2) = 0 \ , \tag{8b}$$

$$(\Gamma_{22} - \Gamma_{33})\Gamma_{12}\Gamma_{13} - \Gamma_{23}(\Gamma_{12}^2 - \Gamma_{13}^2) = 0 \ , \tag{8c}$$

Equations (8a-c) are suitable for calculating the acoustic axes. They represent a system of sixth-order equations for three unknown components of the slowness direction: $n_1$, $n_2$ and $n_3$, where $n_1^2 + n_2^3 + n_3^2 = 1$. The three equations (8a-c) are not independent, hence we solve only two of them. We obtain 72 solutions, which are generally complex-valued. Taking into account that $\pm\mathbf{n}$ describes the same direction, the number of the directions reduces from 72 to 36.

Since eq. (6) yields only 16 acoustic axes, 20 of the 36 directions calculated from (8) must be false and do not describe acoustic axes. In fact, the false directions were incorporated into the solution, when eq. (7) was multiplied by terms $\Gamma_{12}\Gamma_{13}$, $\Gamma_{12}\Gamma_{23}$ or $\Gamma_{13}\Gamma_{23}$ in order to derive eq. (8). Therefore, we should eliminate from the solutions of eq. (8a-c) the directions for which

$$\Gamma_{13} = 0 \text{ and } \Gamma_{23} = 0 \, , \tag{9a}$$

or

$$\Gamma_{12} = 0 \text{ and } \Gamma_{23} = 0 \, , \tag{9b}$$

or

$$\Gamma_{12} = 0 \text{ and } \Gamma_{13} = 0 . \qquad (9c)$$

Equations (9a-c) describe three systems of quadratic equations, each of them having 8 solutions which reduce to 4 directions when omitting different signs of **n**. Hence, we obtained in total 12 false directions. Furthermore, 8 of the 12 false directions appear in eq. (8) twice. Which 8 false directions are doubled, depends on the pair of eq. (8a-c) we actually solve. For example, when solving eq. (8a-b), solutions of eq. (9a) and (9b) are doubled, when solving eq. (8b-c), solutions of eq. (9b) and (9c) are doubled. Hence the total number of the false directions in eq. (8) is 20. This confirms that only 16 acoustic axes can exist in triclinic anisotropy.

### 3. Numerical calculation of positions of singularities

Positions of acoustic axes in triclinic media can be conveniently calculated by solving eqs (8a-c). These are homogeneous polynomial equations of the sixth order for three unknown components $n_1$, $n_2$ and $n_3$ of the unit direction vector **n**. Using the substitution $u = n_1 / n_3$ and $v = n_2 / n_3$, we obtain inhomogeneous polynomial equations of the sixth order for unknowns $u$ and $v$. The roots of the equations can be calculated, for example, using Gröbner bases (Fröberg 1997), implemented in symbolic algebra packages like REDUCE, MAPLE or MATHEMATICA. Solving eqs (8a-c) we obtain 36 solutions, from which we have to exclude 20 false solutions defined by eqs (9a-c). To identify and eliminate the false solutions, we can either solve eqs (9a-c) or we can simply check at which of 36 directions calculated from eqs (8a-c) the Christoffel tensor is non-degenerate. Using this approach we obtain real as well as complex acoustic axes in triclinic media. For media with higher symmetry, we do not use this approach, because it is too complex and it may even fail when the true or false solutions are not isolated. Instead, we use much simpler systems of algebraic equations designed for each specific symmetry (see Khatchevich 1963; Boulanger & Hayes 1998).

The calculation of the real acoustic axes can also be performed using optimization procedures in which we vary the unit direction vector **n** and minimize the difference between two eigenvalues $G$ of the Christoffel tensor $\mathbf{\Gamma}(\mathbf{n})$. In order to get all solutions, we have to run the inversion many times with different initial directions $\mathbf{n}_0$. For example, the initial directions $\mathbf{n}_0$ can cover the hemisphere in a regular grid in spherical angles $\theta$ and $\varphi$. This procedure is applicable for any anisotropy irrespective of its symmetry and it can also yield whether the acoustic axis is *P*-*S*1 or *S*1-*S*2.

## 4. Singularities for homogeneous and inhomogeneous waves

As mentioned above, the 16 acoustic axes in triclinic anisotropy can lie along a real-valued or complex-valued direction **n**. The real-valued acoustic axis corresponds to the propagation of a homogeneous plane wave:

$$u_k(\mathbf{x},t) = A\, g_k \exp\left[-i\omega\left(t - s_j x_j\right)\right], \tag{10}$$

where **u** is the real-valued displacement, $A$ is the scalar real- or complex-valued amplitude and $\mathbf{s} = \mathbf{n}/\sqrt{G}$ is the real-valued slowness vector. Since the Christoffel tensor $\mathbf{\Gamma}$ and its eigenvalues $G$ and eigenvectors **g** are real-valued, the polarization near the acoustic axis is linear. Strictly at the singularity, the polarization is not defined because of the degeneracy of $\mathbf{\Gamma}$.

If the acoustic axis is complex-valued, the corresponding plane wave solution describes an inhomogeneous wave:

$$u_k(\mathbf{x},t) = A\, g_k \exp\left[-i\omega\left(t - s_j x_j\right)\right] = A\, g_k \exp\left(-a_j x_j\right)\exp\left[-i\omega\left(t - p_j x_j\right)\right], \tag{11}$$

where $A$ the scalar real- or complex-valued amplitude, **s** is the complex-valued slowness vector, $\mathbf{s} = \mathbf{n}/\sqrt{G} = \mathbf{p} + i\mathbf{a}$, and **p** and **a** are the real-valued propagation and attenuation vectors (Červený 2004). Subsequently, the Christoffel tensor $\mathbf{\Gamma}$ and its eigenvalues $G$ and eigenvectors **g**, calculated by eqs (1) and (2), are complex-valued, and the polarization near the acoustic axis is elliptical. The ellipticity depends on the direction and magnitude of attenuation vector **a**. Similarly as for homogeneous waves, the polarization is not defined at the acoustic axis because of the degeneracy of $\mathbf{\Gamma}$. Since the problem of the degeneracy is more involved for complex-valued tensors than for real-valued tensors, eqs (6) and (8) do not describe all acoustic axes for inhomogeneous waves, but only the so-called "semisimple" axes (degeneracies). The "non-semisimple" degneracies cannot be investigated by these equations. For more details about the semisimple and non-semisimple degeneracies, see Ting (1996) and Shuvalov (2001).

The polarization properties of homogeneous and inhomogeneous waves near real and complex acoustic axes are exemplified for triclinic anisotropy generated from an isotropic medium with $\lambda = 1$, $\mu = 1$, by adding small perturbations. The elastic parameters are as follows:

$$\mathbf{A} = \begin{bmatrix} 3.004 & 1.004 & 1.004 & 0.004 & 0.002 & -0.001 \\ & 3.004 & 1.002 & -0.002 & -0.001 & 0.001 \\ & & 3.000 & 0.003 & -0.001 & 0.004 \\ & & & 1.001 & 0.001 & -0.001 \\ & & & & 1.000 & 0.003 \\ & & & & & 1.000 \end{bmatrix} \tag{12}$$

The positions of real and acoustic axes over the unit sphere are listed in Table 1 and shown in Fig. 1. The medium contains 6 real and 10 complex acoustic axes. For complex axes, their positions on the sphere are calculated from the real parts of complex directions **n**. Since the complex axes always appear in complex conjugate pairs, Fig. 1b shows 5 instead 10 positions. Figure 2 shows the polarization of homogeneous waves near real acoustic axes No. 10 (see Table 1). The field of polarization vectors displays a singularity with the topological charge –1/2. Figure 3 shows the polarization of inhomogeneous waves near complex acoustic axes No. 6 (see Table 1). The field of polarization vectors displays a singularity with the topological charge +1/2.

**Table 1**. Positions of acoustic axes

| No. | $n_1$ | $n_2$ | $n_3$ |
|---|---|---|---|
| Weak triclinic anisotropy | | | |
| 1 | −0.7839492 | 0.6203156 | 0.0251392 |
| 2 | −0.9332138 − 0.0057073i | −0.3520487 + 0.0349217i | 0.0719272 + 0.0968750i |
| 3 | −0.9332138 + 0.0057073i | −0.3520487 − 0.0349217i | 0.0719272 − 0.0968750i |
| 4 | −0.9295898 | −0.0284564 | 0.3674953 |
| 5 | −0.5147129 | −0.7419284 | 0.4296659 |
| 6 | −0.1551908 − 0.1377317i | −0.9466291 + 0.1102968i | 0.2825049 + 0.2939257i |
| 7 | −0.1551908 + 0.1377317i | −0.9466291 − 0.1102968i | 0.2825049 − 0.2939257i |
| 8 | −0.1776373 + 0.1590932i | 0.8779921 + 0.0594372i | 0.4444937 − 0.0538243i |
| 9 | −0.1776373 − 0.1590932i | 0.8779921 − 0.0594372i | 0.4444937 + 0.0538243i |
| 10 | −0.1655125 | 0.1426004 | 0.9758435 |
| 11 | 0.2658706 | −0.6768519 | 0.6864286 |
| 12 | 0.6709984 + 0.2502343i | −0.5390580 − 0.1446384i | 0.5090948 − 0.4829657i |
| 13 | 0.6709984 − 0.2502343i | −0.5390580 + 0.1446384i | 0.5090948 + 0.4829657i |
| 14 | 0.5716311 | −0.0312721 | 0.8199145 |
| 15 | 0.5849894 + 0.2260697i | 0.5262360 − 0.1537175i | 0.6171409 − 0.0832171i |
| 16 | 0.5849894 − 0.2260697i | 0.5262360 + 0.1537175i | 0.6171409 + 0.0832171i |

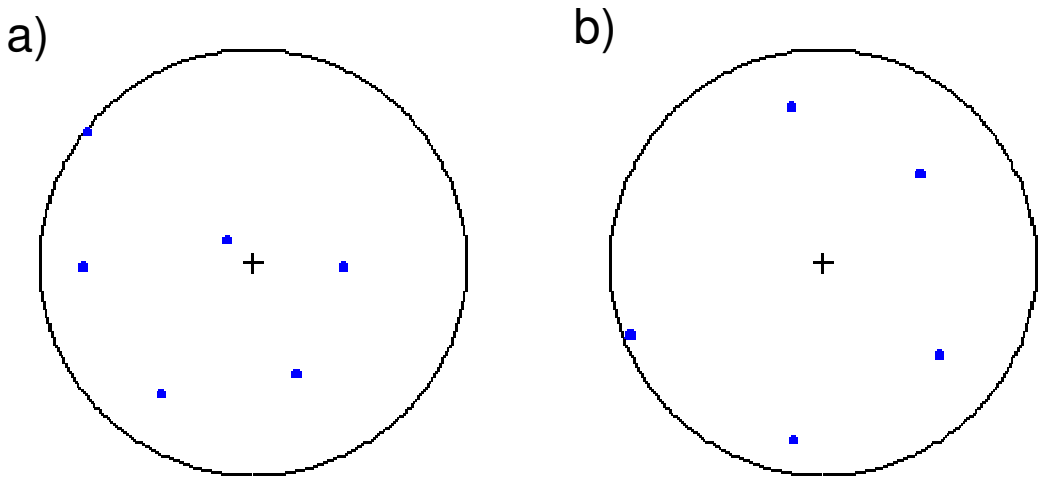


**Figure 1.** Positions of real (a) and complex (b) acoustic axes for a triclinic medium described by eq. (12). Equal-area projection is used.

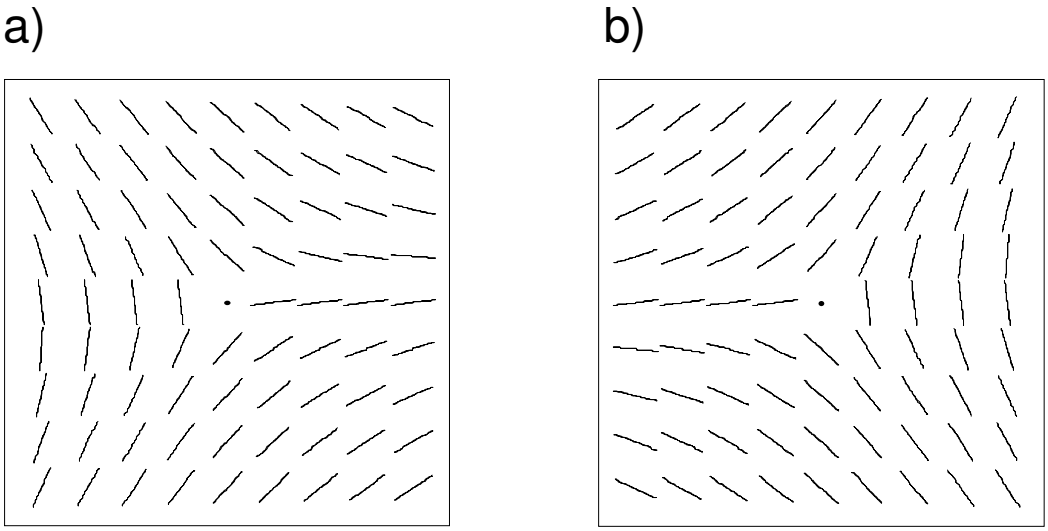


**Figure 2.** Polarization field near a real singularity for (a) S1 wave, and (b) S2 wave. The topological charge of the singularity is -1/2. The dot marks the position of the singularity.

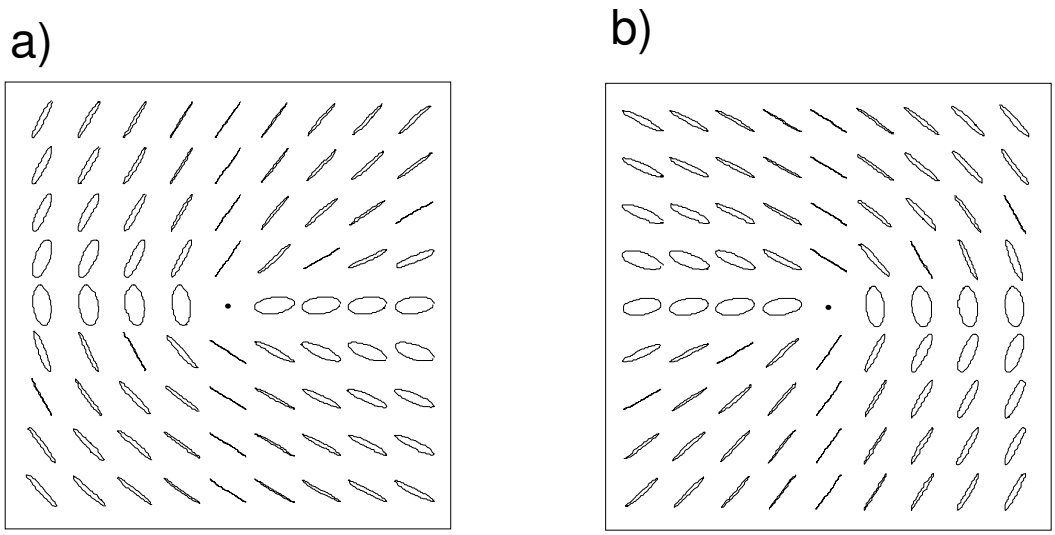


**Figure 3.** Polarization field near a complex singularity for (a) S1 wave, and (b) S2 wave. The topological charge of the singularity is +1/2. The dot marks the position of the singularity.

## 5. Stable and unstable acoustic axes

The 16 acoustic axes can be either single or multiple. The single acoustic axis is stable, because a small perturbation of elastic parameters causes its slight deviation, but the axis cannot split or disappear. The multiple (degenerate) acoustic axis is unstable, because a small perturbation of elastic parameters removes its degeneracy and splits the multiple axis into two or more single axes. The real-valued multiple axis can split into real-valued or complex-valued single axes. The topological charge of the multiple acoustic axis is equal to the sum of the topological charges of split single axes (Darinskij 1994).

Since the probability of existence of the degenerate acoustic axis in triclinic anisotropy is very low, we shall exemplify their properties in cubic anisotropy. This anisotropy is characterized by 4 single real-valued axes in the directions <±1, ±1, ±1> and three multiple real-valued axes <±1, 0, 0>, <0, ±1, 0>, and <0, 0, ±1>. The multiple axes are 4 times degenerate. Hence the total number of real-valued acoustic axes is 7. However, if we consider multiplicities, we obtain 16 real-valued axes, which is the maximum number of axes in anisotropy. This implies that no other complex-valued axis can exist in cubic anisotropy. If we perturb elastic parameters from cubic to triclinic anisotropy, each degenerate axis splits into two real-valued and two complex-valued single axes.

## 6. Frequency of real-valued and complex-valued acoustic axes

Now we address the point what is the balance between the numbers of real- and complex-valued acoustic axes and how this balance depends on strength of anisotropy. For this reason, we randomly generate a triclinic anisotropy and numerically find the numbers of real- and complex-valued acoustic axes. The triclinic anisotropy with elastic parameters $a_{ijkl}$ is obtained by perturbing an isotropic medium in the following way:

$$a_{ijkl} = a^0_{ijkl} + \varepsilon\, a^1_{ijkl}\,, \tag{13}$$

where

$$a^0_{ijkl} = \lambda\delta_{ij}\delta_{kl} + \mu\left(\delta_{ik}\delta_{jl} + \delta_{il}\delta_{jk}\right)\,. \tag{14}$$

Parameters $\lambda$ and $\mu$ define the Lamé coefficients of an isotropic medium, tensor $a^1_{ijkl}$ defines perturbations into triclinic anisotropy, and $\varepsilon$ is a measure of anisotropy strength. Parameters $\lambda$ and $\mu$ are fixed at values $\lambda = 1$, $\mu = 1$, perturbations $a^1_{ijkl}$ are generated randomly with a uniform non-zero probability in the interval $\langle -3, 3\rangle$, and $\varepsilon$ is 0.01 or 1. We checked whether the generated triclinic medium is stable ($\mathbf{\Gamma}$ is positive-definite for any $\mathbf{n}$) or not, and the unstable media were discarded. For $\varepsilon = 0.01$, all the media were stable, for $\varepsilon = 1$, approximately one hundredth of media were stable. To obtain statistically relevant results, the number of randomly generated stable triclinic media is 1000 for each $\varepsilon$.

Fig. 4 shows the frequency of occurrence of triclinic media with a particular number of real or complex acoustic axes. The figure shows that the number of acoustic axes depends on the strength of anisotropy. For weak anisotropy, defined by $\varepsilon = 0.01$, the medium contains most frequently 6 real and 10 complex axes. For strong anisotropy, defined by $\varepsilon = 1$, the most frequent number is 8 for real as well as for complex axes. The media with no real or no complex axis are admissible but they are very rare. To demonstrate their existence we present elastic parameters of two media in Table 2: Anisotropy I with 16 real axes, and Anisotropy II with 16 complex axes. Figure 5 shows the distribution of axes over the sphere, and Table 3 presents their direction vectors **n**. For complex axes, their positions on the sphere are calculated from the real parts of complex directions **n**. Since the complex axes always appear in complex conjugate pairs, Fig. 5b shows 8 instead 16 positions. Anisotropy I was generated in a similar way as other randomly generated triclinic media in the above described numerical tests. Anisotropy II was derived from orthorhombic anisotropy with no real acoustic axes presented by Boulanger and Hayes (1998) by perturbing it into the triclinic anisotropy.

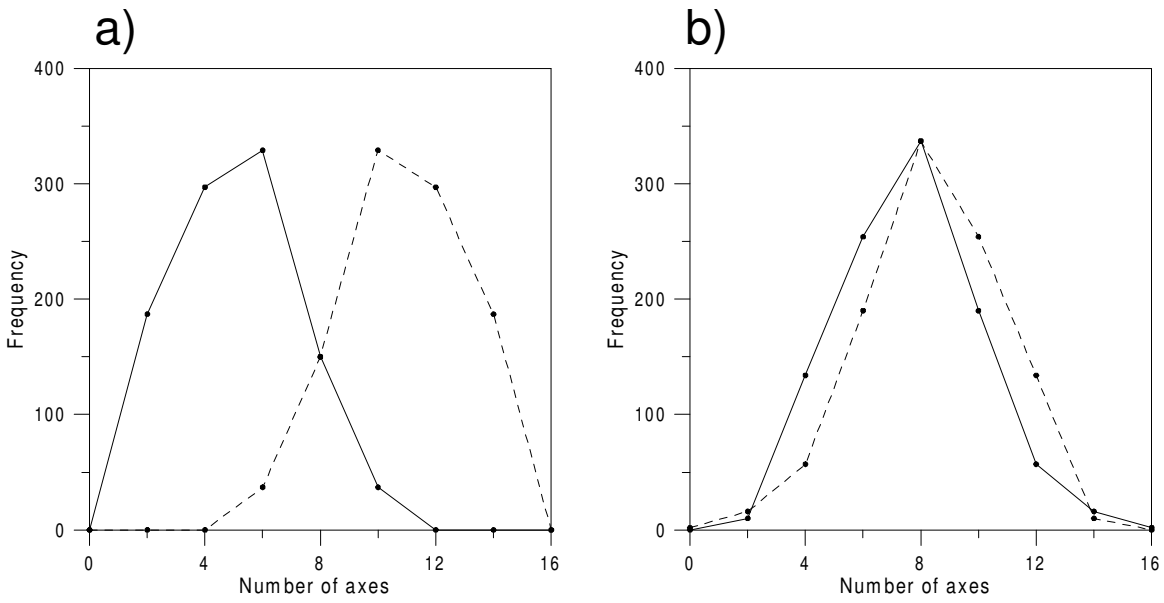


**Figure 4.** Frequency of occurrence of singularities in triclinic medium with varying anisotropy strength. The occurrence of number of real (solid line) and complex (dashed line) singularities for 1000 random triclinic media is shown for anisotropy strength (a) $\varepsilon = 0.01$, and (b) $\varepsilon = 1$.

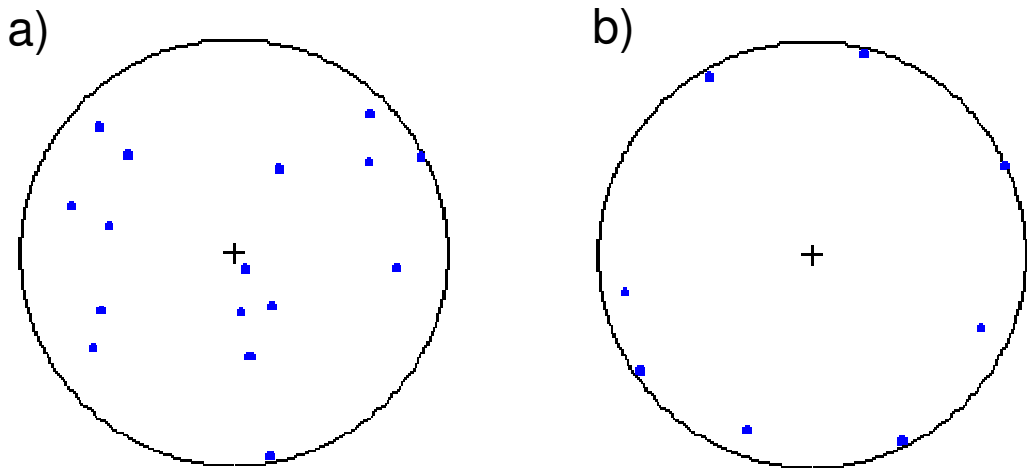


**Figure 5.** Examples of triclinic media with 16 real and no complex singularities (a), and with 16 complex and no real singularities (b). Equal-area projection is used.

**Table 2.** Examples of triclinic anisotropy with 16 real and 16 complex acoustic axes

| | $a_{11}$ | $a_{12}$ | $a_{13}$ | $a_{14}$ | $a_{15}$ | $a_{16}$ | $a_{22}$ | $a_{23}$ | $a_{24}$ | $a_{25}$ | $a_{26}$ | $a_{33}$ | $a_{34}$ | $a_{35}$ | $a_{36}$ | $a_{44}$ | $a_{45}$ | $a_{46}$ | $a_{55}$ | $a_{56}$ | $a_{66}$ |
|---|---|---|---|---|---|---|---|---|---|---|---|---|---|---|---|---|---|---|---|---|---|
| I | 137 | 52 | 57 | -13 | 32 | -20 | 147 | 18 | -6 | 20 | -9 | 100 | 22 | -15 | 5 | 52 | 26 | -7 | 75 | -40 | 30 |
| II | 31 | -5 | -32 | 2 | -2 | -3 | 9 | -11 | 2 | 5 | 4 | 90 | 5 | -1 | -2 | 12 | 1 | -3 | 35 | -2 | 10 |

I – anisotropy with 16 real acoustic axes, II – anisotropy with 16 complex acoustic axes.

**Table 3**. Positions of acoustic axes

| No. | $n_1$ | $n_2$ | $n_3$ |
|---|---|---|---|
| Anisotropy I | | | |
| 1 | 0.1756674 | −0.9828840 | 0.0554974 |
| 2 | −0.7684422 | −0.5215677 | 0.3707607 |
| 3 | 0.1053169 | −0.6432795 | 0.7583533 |
| 4 | −0.7679657 | −0.3340788 | 0.5464612 |
| 5 | 0.0509253 | −0.3858405 | 0.9211588 |
| 6 | 0.2540244 | −0.3455787 | 0.9033531 |
| 7 | 0.9106622 | −0.0855127 | 0.4042050 |
| 8 | 0.0818690 | −0.1112150 | 0.9904184 |
| 9 | −0.7440981 | 0.1575590 | 0.6492249 |
| 10 | 0.2920241 | 0.5228079 | 0.8008706 |
| 11 | −0.8889025 | 0.2511964 | 0.3830829 |
| 12 | −0.6083332 | 0.5714290 | 0.5508171 |
| 13 | 0.7551656 | 0.5067185 | 0.4158860 |
| 14 | −0.7021761 | 0.6610971 | 0.2643846 |
| 15 | 0.6920110 | 0.7020906 | 0.1678967 |
| 16 | 0.8906466 | 0.4536919 | 0.0302025 |
| Anisotropy II | | | |
| 1 | −0.9580463 − 0.0946383i | −0.1915073 + 0.7407283i | 0.2132417 + 0.2400418i |
| 2 | −0.9580463 + 0.0946383i | −0.1915073 − 0.7407283i | 0.2132417 − 0.2400418i |
| 3 | −0.3328521 + 0.2973760i | −0.9148062 − 0.0808199i | 0.2287770 + 0.1094850i |
| 4 | −0.3328521 − 0.2973760i | −0.9148062 + 0.0808199i | 0.2287770 − 0.1094850i |
| 5 | −0.4977868 − 0.1147590i | 0.8640068 − 0.1257704i | 0.0755016 + 0.6826472i |
| 6 | −0.4977868 + 0.1147590i | 0.8640068 + 0.1257704i | 0.0755016 − 0.6826472i |
| 7 | −0.8222318 + 0.0178702i | −0.5656839 + 0.0207860i | 0.0627410 + 0.4216026i |
| 8 | −0.8222318 − 0.0178702i | −0.5656839 − 0.0207860i | 0.0627410 − 0.4216026i |
| 9 | 0.4330259 + 0.0784671i | −0.8999502 + 0.0187197i | 0.0507746 − 0.3374031i |
| 10 | 0.4330259 − 0.0784671i | −0.8999502 − 0.0187197i | 0.0507746 + 0.3374031i |
| 11 | 0.9097104 − 0.0162469i | 0.4150735 + 0.0559198i | 0.0118667 − 0.7104604i |
| 12 | 0.9097104 + 0.0162469i | 0.4150735 − 0.0559198i | 0.0118667 + 0.7104604i |
| 13 | 0.2551059 + 0.1567312i | 0.9653964 − 0.0384612i | 0.0541352 − 0.0526957i |
| 14 | 0.2551059 − 0.1567312i | 0.9653964 + 0.0384612i | 0.0541352 + 0.0526957i |
| 15 | 0.8867209 + 0.2545424i | −0.3880075 + 0.4443174i | 0.2513485 − 0.2120943i |
| 16 | 0.8867209 − 0.2545424i | −0.3880075 − 0.4443174i | 0.2513485 + 0.2120943i |

## 7. Positions of acoustic axes as a function of anisotropy strength

In the next we will study variations in positions of acoustic axes in dependence on anisotropy strength. We show two examples of triclinic media defined by the Lamé coefficients of the isotropic background medium $\lambda = 1$, $\mu = 1$, and by the perturbations $a^1_{ijkl}$:

$$\mathbf{A}^1 = \begin{bmatrix} 1.083 & 1.200 & 0.966 & 0.954 & 0.483 & -0.474 \\ & 1.062 & 0.435 & -0.630 & -0.474 & 0.105 \\ & & 0.000 & 0.684 & -0.570 & 1.017 \\ & & & 0.282 & 0.207 & -0.387 \\ & & & & -0.009 & 0.609 \\ & & & & & 0.000 \end{bmatrix} \tag{15}$$

$$\mathbf{A}^1 = \begin{bmatrix} -0.114 & 0.309 & -1.347 & -0.585 & 1.125 & -1.452 \\ & 0.204 & -0.252 & 0.804 & 1.413 & 1.473 \\ & & 0.000 & 0.867 & -0.183 & -0.003 \\ & & & 0.885 & -0.858 & 0.432 \\ & & & & -1.320 & -0.537 \\ & & & & & 0.000 \end{bmatrix}. \tag{16}$$

The anisotropy strength $\varepsilon$ ranged from -50 to 50 with step of 0.1. Figure 6 shows the positions of the real acoustic axes in the polar plot. The blue/red points show the acoustic axes for stable/unstable media. The figure shows that the acoustic axes are not distributed randomly around a sphere but form lines. The complex acoustic axes display a similar pattern.

## 8. Conclusions

Triclinic elastic anisotropy contains at most 16 isolated acoustic axes. These axes can be real or complex, and single or multiple. If we count both real and complex acoustic axes and their multiplicities, the total number of axes is always 16 regardless of symmetry or strength of anisotropy. The real axes correspond to the degeneracy directions of the real-valued Christoffel tensor, which describes the propagation of homogeneous plane waves.

The complex axes correspond to the semisimple degeneracy directions of the complex-valued Christoffel tensor which describes the propagation of inhomogeneous plane waves. The inhomogeneous waves can possess also other types of acoustic axes called non-semisimple. Real-valued acoustic axis generates a linear polarization in its vicinity, which is singular at the axis. The complex-valued (semisimple) acoustic axis generates an elliptical polarization, which is also singular at the axis. The triclinic anisotropy with 6-10 real acoustic axes is most frequent. A medium with no or 16 real acoustic axes is admissible, but it is very rare.

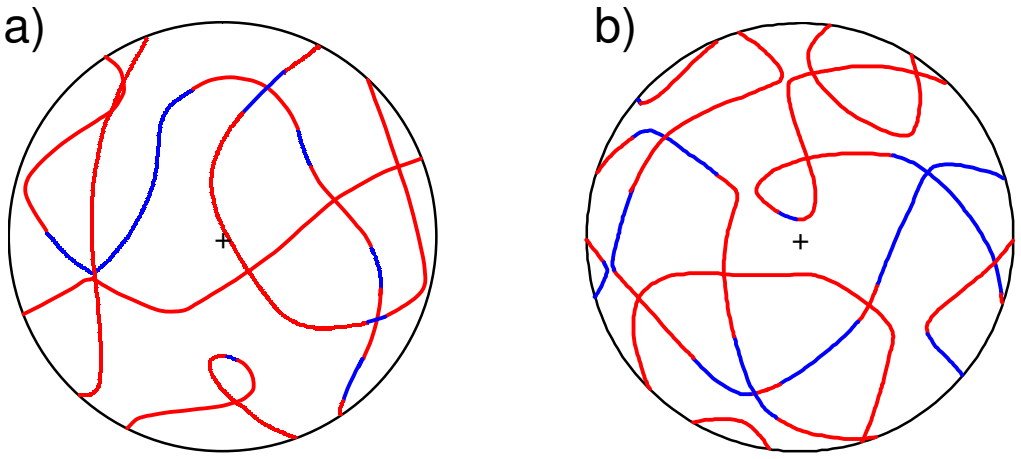


**Figure 6.** Positions of real singularities as a function of anisotropy strength for two triclinic media. (a) The medium is described by elasticity tensor (15). (b) The medium is described by elasticity tensor (16). Blue/red dots denote singularities of stable/unstable media. Equal-area projection is used.

**Acknowledgements**

I thank Vlastislav Červený and Ivan Pšenčík for stimulating discussions on the subject. The work was supported by the Consortium Project SW3D "Seismic waves in complex 3-D structures", and by the Grant Agency of the Academy of Sciences of the Czech Republic, Grant A3012309.

## References


Alshits, V.I. & Lothe, J., 1979a. Elastic waves in triclinic crystals. I. General theory and the degeneracy problem, *Sov. Phys. Crystallogr.*, **24**, 387-392.

Alshits, V.I. & Lothe, J., 1979b. Elastic waves in triclinic crystals. II. Topology of polarization fields and some general theorems, *Crystallography*, **24**, 683-693 (in Russian).

Alshits, V.I., Sarychev, A.V. & Shuvalov, A.L., 1985. Classification of degeneracies and analysis of their stability in the theory of elastic waves in crystals, *J. Exper. Theor. Phys.*, **89**, 922-938 (in Russian).

Boulanger, Ph. & Hayes, M., 1998. Acoustic axes for elastic waves in crystals: theory and applications, *Proc. R. Soc. Lond.*, **A 454**, 2323-2346.

Červený, V., Inhomogeneous harmonic plane waves in viscoelastic anisotropic media, *Stud. Geophys. Geod.*, **48**, 167-186.

Darinskij, B.M., 1994. Acoustic axes in crystals, *Crystallogr. Rep.*, **39**, 697-703.

Every, A.G., 1986. Formation of phonon-focusing caustics in crystals, *Phys. Rev. B*, **34**, 2852-2862.

Every, A.G., 1988. Classification of the phonon-focusing patterns of tetragonal crystals, *Phys. Rev. B,* **37**, 9964-9977.

Fedorov, F.I., 1968. *Theory of Elastic Waves in Crystals*, Plenum Press, New York.

Fröberg, R., 1997. *An Introduction to Gröbner Bases*, John Wiley, New York.

Holm, P., 1992. Generic elastic media, *Physica Scripta*, **T44**, 122-127.

Khatkevich, A.G., 1963. Acoustic axes in crystals, *Sov. Phys. Crystallogr.*, **7**, 601-604.

Khatkevich, A.G., 1977. Classification of crystals by acoustic properties, *Sov. Phys. Crystallogr.*, **22**, 701-705.

Mozhaev, V.G., Bosia, F. & Weihnacht, M., 2001. Oblique acoustic axes in trigonal crystals, *J. Comput. Acoust.*, **9**, 1147-1161.

Musgrave, M.J.P., 1970. *Crystal Acoustics*, Holden-Day, San Francisco.

Musgrave, M.J.P., 1985. Acoustic axes in orthorhombic media, *Proc. R. Soc. Lond.*, **A 401**, 131-143.

Rümpker, G. & Thomson, C.J., 1994. Seismic-waveform effects of conical points in gradually varying anisotropic media, *Geophys. J. Int.*, **118**, 759-780.

Shuvalov, A.L., 1998. Topological features of the polarization fields of plane acoustic waves in anisotropic media, *Proc. R. Soc. Lond.*, **A 454**, 2911-2947.

Shuvalov, A.L., 2001. On the theory of plane inhomogeneous waves in anisotropic elastic media, *Wave Motion*, **34**, 401-429.

Shuvalov, A.L. & Every, G., 1997. Shape of the acoustic slowness surface of anisotropic solids near points of conical degeneracy, *J. Acoust. Soc. Am.*, **101**, 2381-2383.

Ting, T.C.T., 1996. *Anisotropic Elasticity. Theory and Applications*, Oxford University Press, New York.

Vavryčuk, V., 2003a. Parabolic lines and caustics in homogeneous weakly anisotropic solids, *Geophys. J. Int.*, **152**, 318-334.

Vavryčuk, V., 2003b. Behavior of rays near singularities in anisotropic media, *Phys. Rev. B*, **67**, art. no. 54105.

Wolfe, J.P., 1998. *Imaging Phonons. Acoustic Wave Propagation in Solids*, Cambridge University Press, Cambridge.